Int. J. Electrochem. Sci., 13 **(2018)** 11016 – 11023, doi: 10.20964/2018.11.83

International Journal of
ELECTROCHEMICAL
SCIENCE
www.electrochemsci.org

Effect of Deep Eutectic Solvent Composition on the Corrosion Behavior of Electrodeposited Cadmium Coatings on Carbon Steel

Evelin Gutierrez[1,*], *Jose A. Rodriguez*[1], *Julian Cruz-Borbolla*[1], *Yolanda Castrillejo*[2], *Enrique Barrado*[2]

[1] Area Academica de Quimica, Universidad Autonoma del Estado de Hidalgo, Ciudad del Conocimiento, Carretera Pachuca-Tulancingo km 4.5, 42184, Pachuca-Hidalgo, Mexico.
[2] Dpto. de Quimica Analitica, Facultad de Ciencias, Universidad de Valladolid, Paseo de Belen 7, 47011, Valladolid, Spain.
[*]E-mail: evengut10@gmail.com

Received: 15 June 2018 / *Accepted:* 27 August 2018 / *Published:* 1 October 2018

Deep eutectic solvents prepared by mixing choline chloride with urea or thiourea (1:2 molar ratio) were employed to evaluate their effects on the formation of cadmium electrodeposits on a reactive electrode composed of carbon steel 1018. The corrosion protection of carbon steel corresponds to the use of cadmium as a sacrificial anode. Differences in DES affect the electrochemical and corrosion behavior of cadmium.

Keywords: deep eutectic solvent; carbon steel; urea; thiourea; ethylene glycol.

1. INTRODUCTION

Deep eutectic solvents (DES) have been classified as a type of ionic liquid, integrated with nonsymmetric ions, which are obtained by mixing a hydrogen bond acceptor (HBA) as a quaternary ammonium compound with a metallic salt or hydrogen bond donor (HBD) such as primary amines, carboxylic acids, alcohols or imines [1,2]. The mixture of the appropriate components according to the correct molar ratio generates a eutectic, characterized by a melting point lower than both of the individual components, attributed to the charge delocalization occurring between the halide ion and the HBD [3-6].

The most popular ammonium compound employed in DES is choline chloride (ChCl), a biodegradable and nontoxic salt [3]. This salt has been employed in different applications with urea or

ethylene glycol as HBD, with melting points of DES of 12°C and -12.9°C, respectively, enabling use as a solvent at room temperature – an important advantage with respect to typical ionic liquids and traditional organic solvents [2, 7, 8]. DES have utility in electrochemical applications, such as the preparation of metallic alloys, that are not possible in aqueous media [9, 10].

In electrochemistry, deep eutectics have been applied to antioxidant detection [11]; the electrochemical deposition of metals including Ag, Sn, Cr, and Cu; and the formation of sacrificial anodes [3,12,13]. In catalytic processes, these solvents are useful due to properties such as a wide liquid state range, nonflammability and low volatility [14]. DES gained popularity as solvents for nanoparticle synthesis [6], energy storage [15,16] and media for synthesis [17]. Choline chloride mixed with urea (1:2 molar ratio) is a common DES employed in many research fields, mainly owing to the advantages that it presents. The choline chloride-thiourea DES have been employed as media for synthesis or as additives in electrochemical processes, but their application as HBD components in DES is limited [12,18-20].

Taking into account the advantages of employing DES in the formation of metallic electrodeposits, the present paper describes a comparison of cadmium electrodeposit corrosion evolution obtained in two DES, choline chloride-urea (ChCl-U) and choline chloride-thiourea (ChCl-TU) on a carbon steel 1018 surface exposed to a corrosive medium (NaCl 3.0% wt).

2. EXPERIMENTAL

2.1. Reagents

The reagents used in this work were purchased from Sigma-Aldrich, St. Louis, Mo, USA. DES were prepared by mixing ChCl with urea or thiourea at 1:2 molar ratios until a homogeneous and colorless dissolution liquid was observed; the temperature employed for dissolution and electrochemical analysis was 70 °C for ChCl-U, while for the dissolution of ChCl-TU, it was necessary to elevate the temperature to 80°C due to high viscosity. The concentration of $CdCl_2$ (Sigma-Aldrich) on DES was 0.2 $mol \cdot kg^{-1}$, and the prepared solvents were stored at room temperature. Temperature control of DES was accomplished using a recirculating system (Brinkmann Lauda Econoline RE106).

2.2. Electrodes and Instrumentation

The electrochemical studies were performed by employing an electrochemical system (Autolab PGSTAT 30, Eco Chemie B.V., Netherlands) controlled by GPES software version 4.5. The electrochemical characterization was carried out in a three electrode cell. The working electrode consisted of a carbon steel surface AISI 1018 with 0.32 cm^2 of exposed area (0.6-0.9% Mn, 0.15-0.20% C, 0.04% P, 0.05% S, balance Fe), and a platinum wire was employed as an auxiliary electrode. The analysis was developed using an Ag/AgCl (MW-2021 Basi, West Lafayette, IN, USA) reference electrode. The carbon steel surface was renewed at the end of each analysis by sequential abrasion

using emery paper of 80, 600 and 1200 grid. After renewal, the surface was cleaned with acetone and washed with deionized water (Milli-Q Plus system, Millipore, Bedford, MA, USA).

Cyclic voltammetry was carried out moving from open circuit potential to cathodic potential at a scan rate of 10 $mV \cdot s^{-1}$. The potentiodynamic polarization of Cd electrodeposited on a carbon steel surface and an unmodified surface was performed in NaCl aqueous solution (3% wt), prepared in deionized water obtained from a Milli-Q Plus system (Millipore, Bedford, MA, USA) with a resistivity not less than 18.2 MΩ. An anodic sweep was applied in the potential interval of ±100 mV (scan rate of 1 $mV \cdot s^{-1}$) around the open circuit potential.

3. RESULTS AND DISCUSSION

3.1. Electrochemical behavior of Cd(II) in DES

In Figure 1 (a,b), the cyclic voltammograms performed in ChCl-U and ChCl-TU with and without $CdCl_2$ (0.2 mol kg^{-1}) are shown. The potential window obtained on a carbon steel electrode in the two DES has a cathodic limit of about -1.4 V (*vs.* Ag/AgCl) and can be observed in a discontinuous black line in Figure 1 (a,b). The cathodic limit in the electrochemical window of DES that contains choline chloride has been associated with the formation of molecular hydrogen caused by the presence of water [21], which is associated with the hygroscopic nature of DES components.

The voltammograms show a reduction signal attributed to the reduction of Cd(II) to Cd at -1.0 and -1.2 V (*vs.* Ag/AgCl) in ChCl-U and ChCl-TU, respectively. A single signal is observed during the anodic sweep at -0.7 V and -0.8 V (*vs.* Ag/AgCl) for DES ChCl-U and ChCl-TU, respectively. Differences in potential can be attributed to increases in viscosity of the DES that involve a decrease in convection and an increase in resistance [22]. A positive displacement of the potential of the reduction peak and increases in current on DES has been associated with the ease of nucleation and growth of deposits on a surface [23].

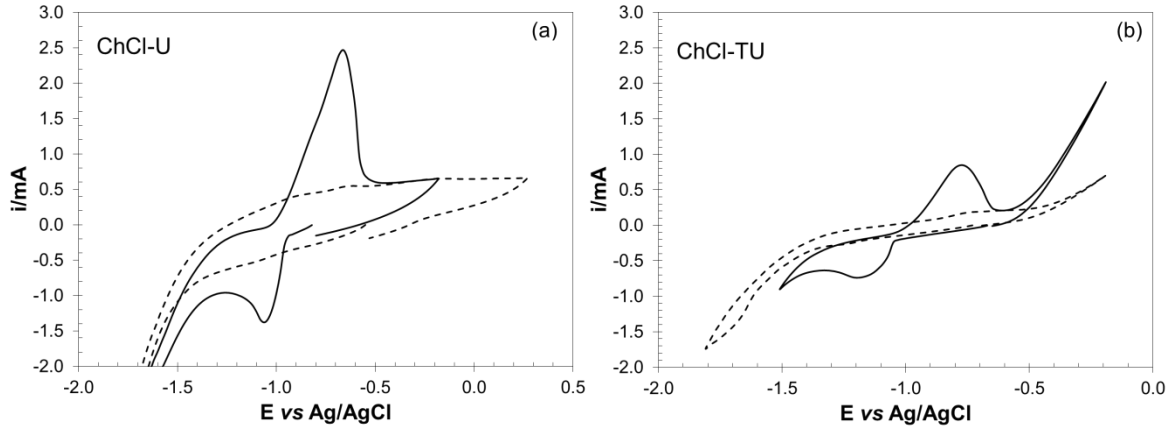

Figure 1. Cyclic voltammograms obtained with a Cd(II) solution (0.2 $mol \cdot kg^{-1}$) on a carbon steel 1018 electrode (S=0.32 cm^2) in DES (a) ChCl-U and ChCl-TU. Sweep rate 10 $mV \cdot s^{-1}$.

The diffusion coefficient is associated with electroactive species movement in different media; in DES, the diffusion coefficient is related to viscosity and temperature [24,25]. The determination of the diffusion coefficient can be realized by employing different electrochemical techniques including voltammetry, convolutive potential sweep voltammetry, chronoamperometry and chronopotentiometry [26,27].

The diffusion coefficient is determined by employing peak current and potential values, but the main disadvantage is that not all the information is used. An appropriate alternative is the analysis by convolution of a series of cyclic voltammograms. In the convolution method, the voltammogram data are transformed into intensity-potential curves. The diffusion coefficient is obtained by employing the values of limit current *m**, described by the equation:

$$m^*=nFSC_0D^{1/2}$$

where C_0 is the concentration (mol·cm^{-3}), D the diffusion coefficient of electroactive species (cm^2·s^{-1}), S is the electroactive area of the work electrode (cm^2), F the Faraday constant, and n is the electron number involved in the electrochemical reaction [28]. In Figure 2, there are examples of voltammograms and convoluted signals obtained in DES ChCl-U (a) and ChCl-TU (b), which were employed for determination of diffusion coefficient in two solvents. The diffusion coefficient values of Cd(II) were 3.3(±0.4)×10^{-7} cm^2·s^{-1} and 1.5(±0.7)×10^{-7} cm^2·s^{-1} in ChCl-U and ChCl-TU, respectively. These values are lower than those obtained in aqueous media, 0.6×10^{-5} to 0.8×10^{-5} cm^2·s^{-1} [29], and similar to diffusion coefficients obtained in ChCl-based DES for other ions. The value obtained in ChCl-TU is lower than that for ChCl-U: this difference is attributed to the viscosity and water content of the media [25]. It has been proposed that low diffusion coefficient values are associated with lower thickness of the electrodeposit coating, which negatively affects their corrosion protection [13,30].

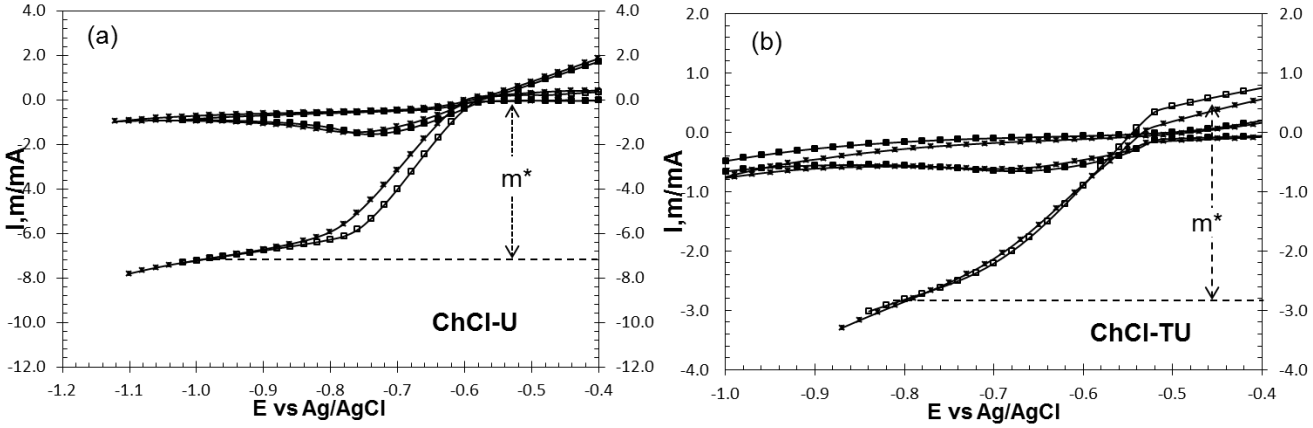

Figure 2. Examples of cyclic voltammograms and their corresponding convoluted curves, obtained with a Cd(II) solution (0.2 mol·kg^{-1}) on a carbon steel electrode (S=0.32 cm^2) in DES (a) ChCl-U and (b) ChCl-TU. The diffusion coefficient was obtained over the sweep rate interval from 10 to 60 mV·s^{-1}.

3.2. Electrochemical nucleation of Cd at the carbon steel electrode

The nucleation process of Cd(II) on a carbon steel electrode was analyzed by employing chronoamperometry. A series of experiments was executed, ranging from an initially selected potential

value where no reduction of cadmium deposition takes place to appropriate negative potentials that cause the nucleation and growth processes of Cd. Once every deposit was complete, the Cd was removed from the surface of the working electrode by anodic polarization.

Current-time transients obtained by the performed experiments are included in Figure 3. On current-time lines obtained in two DES, it is possible to observe the characteristic zones corresponding to nucleation and growth processes. The applied step potential causes an initial sharp current spike associated with double layer charge; this behavior is followed by a rising current resulting from an increase of electroactive surface due to formation and growth of Cd nuclei on the working electrode surface, and the current reaches a characteristic maximum value (j_{max}) at a corresponding time (t_{max}), after which the current decreases as a result of a controlled diffusion process.

In Figure 3, it is possible to observe that the time required to reach maximum current decreases as a result of an imposition of higher negative overpotentials. To define the Cd nucleation type, dimensionless experimental current-time transients were constructed by employing chronoamperometry data obtained in two DES. Experimental data were compared with theoretical dimensionless current-time transients from Scharifker and Hills models [31]. In Figure 3, dimensionless experimental data obtained by chronoamperometry and theoretical current-time transients for both types of nucleation are represented together.

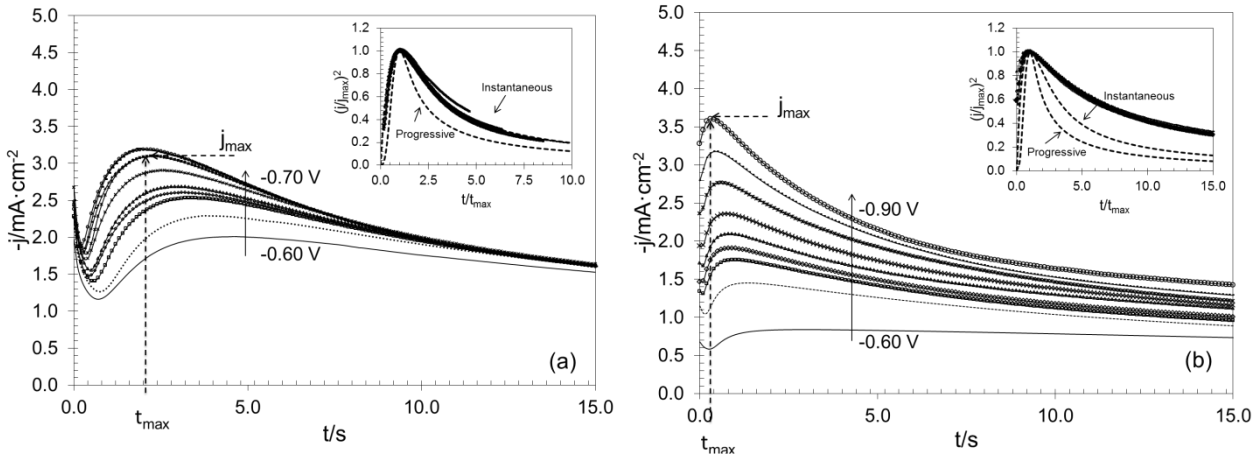

Figure 3. Current-time transients obtained with a Cd(II) solution (0.2 mol·kg^{-1}) on a carbon steel electrode (S=0.32 cm^2). Comparison of the dimensionless curves for instantaneous and progressive nucleation. (a) ChCl-U and (b) ChCl-TU.

The comparison in the DES ChCl-U shows that Cd follows a behavior of instantaneous nucleation. The process in the DES ChCl-TU shows a tendency for a mechanism of instantaneous nucleation. Instantaneous nucleation has been described as an immediate activation of a small number of sites for nucleation, while progressive nucleation corresponds to a slow and continuous process with the formation of a large number of active sites [32,33].

It has been shown that imposed potential and high temperatures cause the acceleration of nuclei growth and that, consequently, a thicker electrodeposit was obtained [12]. A deviation in the

nucleation mechanism is related to the co-reduction of the electrolyte medium, affecting the morphology of the deposit and the corrosion behavior [23].

3.3. Polarization analysis

Cd electrodeposits formed by employing the DES ChCl-U and ChCl-TU (-0.85 V *vs.* Ag/AgCl, 10 min) on a carbon steel surface were immersed in a corrosive medium (NaCl, 3% wt). The comparison of corrosion behavior was analyzed by potentiodynamic polarization. Figure 4(a) shows the Tafel curves of the modified and unmodified surfaces at time 0 and 6 h. The corrosion potential observed at the Cd modified surface (-0.82 V when ChCl-U was used and -0.80 V in the case of ChCl-TU) is lower than that obtained with an unmodified surface (-0.51 V). The corrosion potential (E_{corr}) and density corrosion current (j_{corr}), measured each hour during six hours, are listed in Table 1. With respect to corrosion current, the value obtained at modified carbon steel is higher: this behavior is characteristic of sacrificial anodes [13,34,35].

On the other hand, the corrosion potential (E_{corr}) changes in the positive direction during the first hour of exposure to corrosive solution (Figure 4(b)), and then, the corrosion potential remains constant during the next six hours. This behavior can be attributed to the presence of cadmium on the surface, followed by the formation of cadmium corrosion products. The electrodeposited cadmium and the products of corrosion formed by exposure to the aggressive environment are useful to protect carbon steel. Similar behavior involving resistance to corrosion has been observed in Ni and Ni-Si layers, in which the presence of Si improves resistance to corrosion [23].

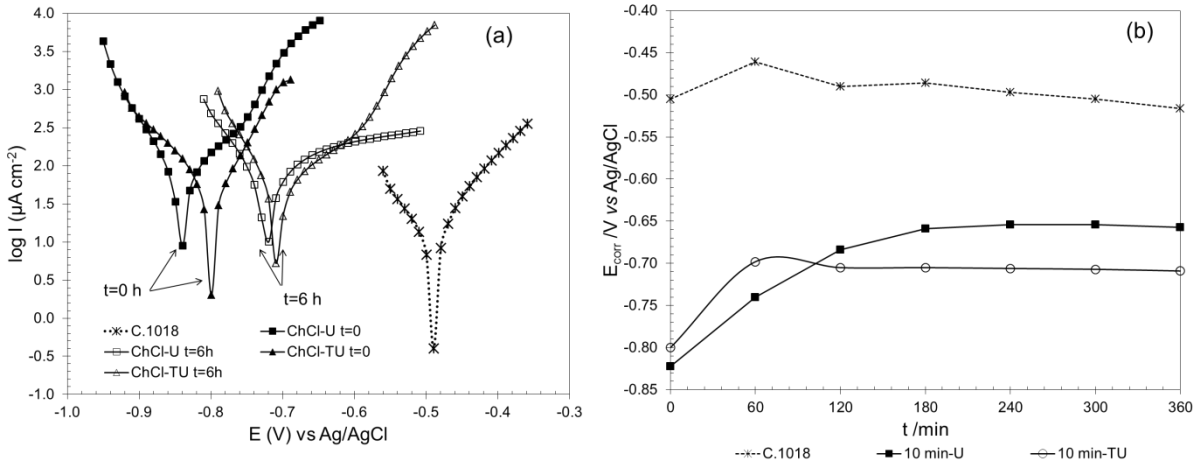

Figure 4. (a) Potentiodynamic polarization of cadmium electrodeposits formed in ChCl-U, ChCl-TU and carbon steel 1018 (C.1018) immersed in NaCl (3.0%wt). (b) Variation of corrosion potential *vs.* exposition time of cadmium electrodeposits and unprotected surface.

Table 1. Electrochemical parameters obtained from polarization curves of unprotected surface (C.1018) and cadmium coatings formed in ChCl-U and ChCl-TU.

	C.1018		ChCl-U		ChCl-TU	
Time (h)	**E_{corr} (V)**	**j_{corr} ($\mu A \cdot cm^{-2}$)**	**E_{corr} (V)**	**j_{corr} ($\mu A \cdot cm^{-2}$)**	**E_{corr} (V)**	**j_{corr} ($\mu A \cdot cm^{-2}$)**
0	-0.51	18.99	-0.82	70.38	-0.80	37.56
1	-0.46	10.69	-0.74	126.25	-0.70	61.41
2	-0.49	21.85	-0.68	90.94	-0.71	62.88
3	-0.49	20.68	-0.66	81.09	-0.71	59.03
4	-0.50	36.92	-0.65	62.66	-0.71	55.69
5	-0.51	27.80	-0.65	66.34	-0.71	58.03
6	-0.52	35.03	-0.66	60.56	-0.71	58.63

4. CONCLUSIONS

The formation of electrochemical deposits is influenced by DES characteristics including composition, viscosity, temperature and electrical conductivity. DES ChCl-U and ChCl-TU allow the formation of cadmium electrodeposits. The nucleation mechanism is more evident in ChCl-U and is associated with an increase in viscosity of ChCl-TU. The corrosion behavior is similar in cadmium electrodeposits formed in both DES. Even though the diffusion coefficient of ChCl-TU is lower than that obtained in ChCl-U and aqueous media, it is possible to use DES during Cd electrodeposition.

ACKNOWLEDGEMENTS
The present work was supported by Junta de Castilla y Leon (Project VA171U14).

References

1. E.L. Smith, A.P. Abbott and K.S. Ryder, *Chem Rev*., 114 (2014) 11060.
2. C.A. Nkuku and R.J. LeSuer, *J. Phys. Chem* B, 111 (2007) 13271.
3. A. Abo-Hamad, M. Hayyan, M.A. AlSaadi and M.A. Hashim, *Chem. Eng. J.,* 273 (2015) 551.
4. F.S. G. Bagh, M.K.O. Hadj-Kali, F.S.Mjalli, M.A. Hashim and I.M. AlNashef, *J. Mol. Liq*., 199 (2014) 344.
5. D.Z. Troter, Z.B. Todorovic, D.R. Dokic-Stojanovic, O.S Stamenkovic and V.B. Veljkovic, *Renewable and Sustainable Energy Reviews,* 61 (2016) 473.
6. S.H. Gage, D.A. Ruddy, S. Pylypenko and R.M. Richards, *Catal. Today,* 306 (2018) 9.
7. D. Lloyd, T. Vainikka, L. Murtomäki, K. Kontturi and E. Ahlberg, *Electrochim. Acta,* 56 (2011) 4942-4948.
8. X. Xie, X. Zou, X. Lu, C. Lu, H. Cheng, Q. Xu and Z. Zhou, *Appl. Surf. Sci*., 385 (2016) 481.
9. G. Saravanan and S.Mohan, *J. Alloys Compd*., 522 (2012) 162.
10. J.M. Hartley, C. Ip, G.C.H. Forrest, K. Singh, S.J. Gurman, K.S. Ryder, A.P. Abbott and G. Frisch, *Inorg. Chem*., 53 (2014) 6280.
11. F.J. Vicente, M. Espino, M.A. Fernandez, J. Raba and M.F. Silva, *Anal. Chim. Acta,* 936 (2016) 91.
12. L.I.N. Tomé, V. Baiao, W. da Silva and C.M.A. Brett, *Applied Materials Today,* 10 (2018) 30.
13. E. Gutiérrez, J.A. Rodríguez, J. Cruz-Borbolla, Y. Castrillejo and E. Barrado, *Int. J. Electrochem. Sci.,* 12 (2017) 8860.
14. X. Pei, Z. Gao-Wei, Z. Min-Hua, L. Ning and L. Wen-Yong, *Bioresources and Bioprocessing,* 4 (2017) 1.

15. M.H. Chakrabarti, F.S. Mjalli, L.M. AiNashef, M.A. Hashim, M.A. Hussain, L. Bahadori and C.T.J. Low, *Renew. Sust. Energ. Rev*., 30 (2014) 254.
16. L. Bahadori, M.A. Hashim, N.S.A. Manan, F.S. Mjalli, I.M. Al-Nasher, N.P. Brandon and M.H. Chakrabarti, *J. Electrochem Soc*., 163 (2016) A632.
17. H. Zhao and G.A. Baker, *J. Chem. Technol. Biotechnol*., 88 (2013) 3.
18. C. Mukesh, D. Mondal, M. Sharma, K. Prasad, *Carbohydr. Polym*., 103 (2014) 466.
19. Y.L. Zhu, Y. Katayama, T. Miura, *Electrochim. Acta*, 85 (2012) 622.
20. R. Costa, M. Figueiredo, C.M. Pereira, F. Silva, *Electrochim. Acta*, 55 (2010) 8916.
21. M. Pölzler, A.H. Whitehead and B. Gollas, *ECS Transactions,* 25 (2010) 43.
22. S. Salomé, N.M. Pereira, E.S. Ferreira, C.M. Pereira and A.F. Silva *J. Electroanal. Chem*., 703 (2013) 80.
23. R. Li, Y. Hou and J. Liang, *Appl. Surf. Sci*., 367 (2016) 449.
24. M.R. Bermejo, E. Barrado, A.M. Martínez, Y. Castrillejo, *J. Eletroanal. Chem*., 617 (2008) 85.
25. S. Fryars, E. Limanton, F. Gauffre, L. Paquin, C. Lagrost, P. Hapiot, *J. Electroanal. Chem*., 819 (2018) 214.
26. E. Barrado, R.A.S. Couto, M.B.Quinaz, J.LF.C. Lima and Y. Castrillejo, *J. Electroanal. Chem*., 720-721 (2014) 139.
27. A. Mandroyan, M. Mourad-Mahmoud, M.L. Doche and J. Hihn, *Ultrason. Sonochem*., 21 (2014) 2010.
28. A.M. Martínez, Y. Castrillejo, E. Barrado, G.M. Haarberg and G. Picard, *J. Electroanal. Chem*., 449 (1998) 67.
29. S. Kariuki and H.D. Dewald, *Electroanal.,* 8 (1996) 307.
30. M. Jeong, T. Yokoshiva, H. Nara, T. Momma, T. Osaka, *RSC,* 4 (2014) 26872.
31. Q. Chu, J. Liang and J. Hao, *Electrochim. Acta,* 115 (2014) 499.
32. H. Yang and R.G. Reddy, *Electrochim. Acta,* 147 (2014) 513.
33. Y. Castrillejo, A.M. Martinez, M. Vega, E. Barrado and G. Picard, *J. Electroanal. Chem*., 397 (1995) 139.
34. A.P. Yadav, H. Katayama, K. Noda, H. Masuda, A. Nishikata and T. Tsuru, *Corros. Sci*., 49 (2007) 3716.
35. A. Conde, M.A. Arenas, J.J. de Damborenea, *Corros. Sci*., 53 (2011) 1489.